Stability of medium-sized neutral and charged silicon clusters

Bao-xing Li
Department of Physics, and Microfluidic Chip Institute, Hangzhou Teachers' College, Hangzhou, Zhejiang 310012, China
(Received 1 December 2004; revised manuscript received 21 March 2005; published 10 June 2005)

Using the full-potential linear-muffin-tin-orbital molecular-dynamics method based on the single-parent evolution algorithm, we have studied the stability for the medium-sized neutral, anionic, and cationic silicon clusters in detail. We have found the ground state structures of Si_n ($n=26-30$). Our calculated results suggest that the compact structures containing interior atoms begin to compete for the ground state structures with the stacked prolate structures from $n=24$. The prolate structures transit into the spherical compact structures at $n=27$ for neutral silicon clusters, whereas the transition size occurs at $n=28$ for anionic and cationic silicon clusters. Starting from $n=29$, the stable structures with larger binding energies are basically the compact spherical structures. The results are in excellent agreement with the related experiments.

DOI: 10.1103/PhysRevB.71.235311 PACS number(s): 71.10.−w, 36.40.−c, 71.20.−b, 31.15.−p

I. INTRODUCTION

Silicon is a very important semiconductor material that has attracted considerable interest. In bulk silicon, each silicon center is sp^3 hybridized and bonded to four other silicon atoms so as to locally form a regular tetrahedron. However, experimental and theoretical investigations on the ground state structures for small silicon clusters have brought to light such a fact that they are not pieces of silicon crystal.[1,2] The small silicon clusters are largely unrelated to bulk silicon in their structures and builds them atom-by-atom into a series of unique molecular structures.

Up to now, an enormous effort has been devoted to determining the structures of the silicon clusters. Although some progress has been made, the structures with only $n\leqslant 7$ (except $n=5$) have been confirmed by experiments.[3–5] Theoretical investigations show that their ground state structures are polyhedrons for the small silicon clusters ranging from 5 to 13.[2,6–16] The structures with $n\leqslant 10$ have been universally accepted.[11] Starting from $n=14$, the stacked prolate structures become more stable than other structures. After $n=19$, some near-spherical shapes without interior atoms begin to show high stability.[15,17] Starting from $n=24$, the near-spherical structure with interior atoms would compete for the ground state structures with the prolate structures. However, up to $n=25$, the stacked prolate structures are still the most stable. An essential feature of the stacked prolate structures is that they are built on a structural motif consisting of a stack of Si_9 tricapped trigonal prisms (TTP).[2,6,17] Besides the results above, Pouchan *et al.* investigated the relationship between the polarizability, stability, and the geometry of small-size silicon clusters by the density functional theory methods.[11,13] They have shown that the polarizability is directly related to the size of the energy gap between symmetry-compatible bonding and antibonding molecular orbitals, and the averaged Si—Si distances and the standard deviation of the Si—Si distances correlate remarkably well with the binding energy of the clusters and the highest occupied molecular orbital (HOMO)-lowest unoccupied molecular orbital (LUMO) gap, respectively.

For the larger silicon clusters with $n\geqslant 26$, only a few reports can be found. Kaxiras and co-worker had proposed two distinct types of structures,[9,10] theoretically. The first type corresponds to the prolate structures. They consist of puckered sixfold rings of atoms, stacked along a central axis of threefold rotational symmetry and capped by one atom at either end. The second type is a series of more compact geometries with many interior atoms. They performed first-principles total-energy calculations for clusters of both types over the size range $n=20-33$ atoms. Their results suggest that there is a transition in the shape of the most stable clusters as the atomic number increases. For the smaller clusters, the prolate structures are more favorable, while the larger clusters prefer the compact structures. The crossover between the prolate and spherical shapes lies in the range $24\leqslant n\leqslant 28$. Grossman and Mitáš had discovered a family of stable elongated Si_n ($n\leqslant 50$) clusters built from a simple stacking scheme by local density approximation molecular cluster calculations.[18] The structures can be obtained by stacking triangles of atoms on a common axis and adding one or two caps. Sieck and co-workers had investigated the structure of low energy neutral silicon clusters with 25, 29, and 35 atoms with a density-functional based tight-binding approach.[19] They found different dominant shapes in the set of low energy clusters for each size. For a neutral Si_{25} cluster, both prolate and spherical structures with large binding energies exist. For silicon clusters with 29 or 35 atoms, the low-energy isomers exhibit a spherical shape. Experimentally, Jarrold and Constant had measured the mobilities of size-selected silicon cluster ions in helium using injected-ion drift-tube techniques.[20] Their results suggest that a major structural transition occurs for clusters with around 27 atoms.

Despite the progress that has been made, however, little is known about their ground state structures for the neutral and ionic silicon clusters ranging from 26 to 30. To our knowledge, no systematic theoretical investigation on searching the ground state structures of Si_{26-30} neutral and ionic clusters has been reported. In this paper, we have performed calculations on the structures for the medium-sized neutral, anionic, and cationic silicon clusters in detail by using the full-potential linear-muffin-tin-orbital molecular-dynamics (FP-LMTO-MD) method based on the single-parent evolution algorithm. Our aim is to explore growth attributes for silicon

clusters and find their ground state structures.

This paper is organized as follows. Section II contains a brief description of the improved FP-LMTO-MD method used. In Sec. III we present calculated results and detailed discussions. The conclusions are given in Sec. IV.

II. METHOD

An unbiased global search for the ground state structures of silicon clusters with $n \leqslant 18$ had been performed successfully by means of a genetic algorithm.[2] The larger clusters cannot be obtained using the genetic algorithm.[2] Recently, Rata *et al.* have successfully developed a single-parent evolution algorithm to find the lowest-energy structures for silicon clusters with $n=13-23$.[21] They found a number of new isomers, which are more stable than any structures previously reported and have properties in much better agreement with experimental data. The single-parent evolution algorithm involves only a single parent, while the previous genetic algorithm contains multiple parents. In this new algorithm, some geneticlike operations are employed in order to add diversity. We have combined the single-parent evolution algorithm with the FP-LMTO method to investigate the ground state structures for Si_n ($n=11-25$) clusters.[6] Some satisfying results have been obtained. The FP-LMTO method[22–25] is a self-consistent implementation of the Kohn-Sham equations in the local-density approximation. In this method, space is divided into two parts: nonoverlapping muffin-tin (MT) spheres centered at the nuclei and the remaining interstitial region. The electron wave functions are expanded in terms of muffin-tin orbitals.[26] The LMTOs are augmented Hankel functions, and are augmented only inside the MT spheres rather than in the interstitial region.[26–28] All MT sphere radii for Si are taken as 2.0 a.u. The LMTO basis sets include *s*, *p*, and *d* functions on all spheres. Its potential and density are expressed as a linear combination of Hankel functions. The details of how the molecular dynamics can be performed are described in Refs. 24 and 25. The geometries obtained are true local minima of the total energy by means of the full-potential linear-muffin-tin-orbital molecular-dynamics (FP-LMTO-MD) method based on the single-parent evolution algorithm. The reliability of the method applied for the small silicon clusters has been tested.[29] Some comparisons with other sophisticated methods have been also made.[29] The results obtained are in good agreement with the related experiments.

III. RESULTS AND DISCUSSIONS

Employing the sophisticated molecular dynamics method mentioned above, we have obtained some important information on the silicon clusters within the scope of structural transition. The first four most stable structures are shown as in Fig. 1. Even though the bond lengths and bond angles between the neutral clusters and their corresponding ions are different, their basic configurations are similar. For simplicity, their structures are shown in one identical chart. The English alphabet n, a, and c in parentheses represent the neutral, anionic, and cationic silicon clusters, respectively. The Arabic alphabets in brackets correspond to their binding energy ordering. Their binding energies and point group are listed in Tables I–III, respectively.

For Si_{26} and its ion clusters, five different structures with larger binding energies are shown as 26A, 26B, 26C, 26D, and 26E in Fig. 1. The first four structures are prolate, while the last one is compact. Three of the four prolate structures include a Si_9 tricapped trigonal prism (TTP) subunit at least. 26A is the most stable for a neutral Si_{26} cluster. It has the same initial configuration as 26C. Structural distortion makes cluster ion structure 26C differ from 26A. 26B is the second most stable for a neutral cluster, but it is the most stable for cluster ions. It is found from 26D and 26E that the neutral and cationic clusters have the same energy ordering, whereas the ordering reverses for the anionic cluster. The energy differences between the most stable and the fourth most stable structures are 1.46, 1.21, and 0.34 eV for neutral Si_{26}, positive Si_{26}^+ ion, and negative Si_{26}^- ion, respectively. Therefore the energy ordering for the anionic cluster is easily different from that of the neutral or cationic clusters.

For the silicon clusters with 27 atoms, the situation is different. First, the prolate 27A and the near-spherical 27B are degenerate for the Si_{27} cluster. 27 is structural transition size for the neutral cluster. For its cationic cluster, the energy difference between 27A and 27B is only 0.05 eV. They have almost the same stability. Second, the ground state structure of Si_{27}^+ is a stacked structure consisting of three TTP subunits, which is different from that of Si_{26} or Si_{26}^-. Third, there are three compact structures among five different structures. Obviously, the stability of the compact structures increases. Fourth, the lowest energy structure of a Si_{27} anionic cluster is a perfectly prolate structure shown as 27E in Fig. 1, which differs from those of neutral and cationic Si_{27} clusters.

All three ground state structures of Si_{28}, Si_{28}^-, and Si_{28}^+ correspond to 28A, which is a near-spherical compact configuration with D_{2h} symmetry. The three clusters with different electron number have different energy ordering in the other five structures. For the neutral Si_{28} and cationic Si_{28}^+, the second and third lowest energy structures are compact although their energy ordering is different. Their fourth stable structures correspond to different prolate configurations. The prolate structures 28C and 28F still lie in the second and third stable places for the anionic Si_{28}^-. 28C is obtained by capping an atom on the end of 27E, which is the ground state structure of Si_{27}^-.

Starting from $n=29$, the compact structures become more favorable. Except for 29D, which is a prolate structure corresponding to the fourth stable structure of Si_{29}^-, all the other structures are near-spherical compact. Si_{29} and Si_{29}^+ have the same energy ordering, but not for Si_{29}^-.

When $n=30$, a similar conclusion can be obtained. 30A, 30B, 30C, and 30D with large binding energies are compact structures, while the prolate structure 30E is only the fourth stable structure of Si_{30}^-. 28A, 29A, and 30A in Fig. 1 are the ground state structures of Si_{28}, Si_{29}, and Si_{30}, respectively. They have the same symmetry C_{2v}. Although the coordination numbers of the interior atoms in the three structures are high (up to 8 or 9), most of the other outer atoms are tetrahedrally coordinated. As the atomic number increases, the coordination numbers of the interior atoms would decrease.

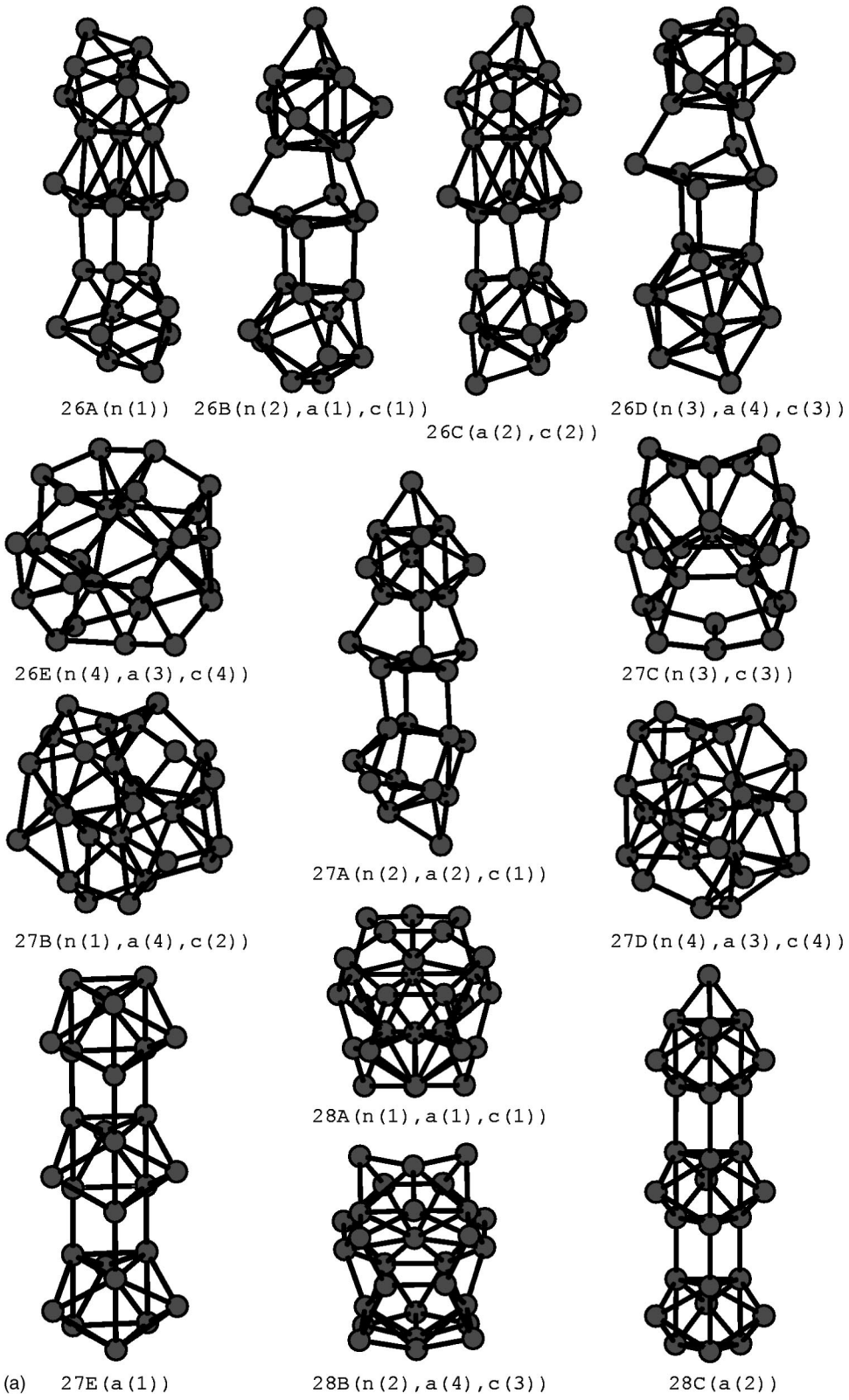

FIG. 1. The first four most stable structures for the silicon clusters with $n=26-30$. The letters n, a, and c in parentheses represent the neutral, anionic, and cationic silicon clusters, respectively. The Arabic alphabets in brackets correspond to their binding energy ordering.

It is found from Fig. 1 that the energy ordering of many cationic clusters is the same as that of the neutral clusters, but only a few for the anionic clusters. Our calculations suggest that many of the cations usually have similar configurations to the neutral clusters. But, generally, the anions have significant structural distortion compared with the cations. The different distortions result from the different polarization of electron spin charge density. In fact, because many of the structures for the neutral clusters have electronic structures with a highest doubly occupied orbital, removal of an electron from the highest occupied molecular orbital (HOMO) does not perturb the energy gap E_g between HOMO and

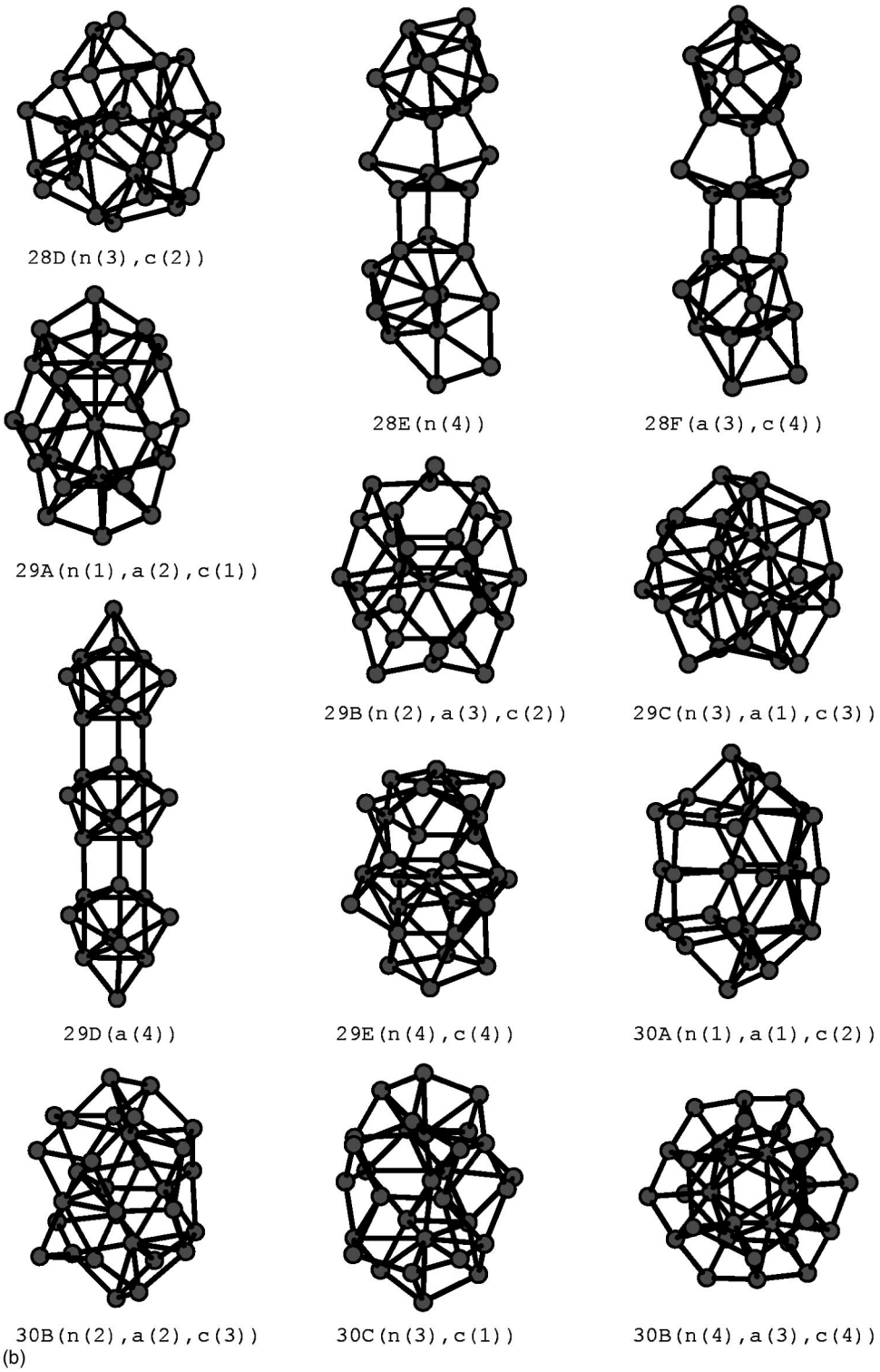

(b)

FIG. 1. (*Continued*).

LUMO (the lowest unoccupied molecular orbital) significantly. But, because the additional electron in the anions goes into the lowest unoccupied orbital, its Fermi level changes definitely. The HOMO-LUMO gap is, by and large, often directly related to polarizability in a cluster system.[11] According to simple perturbation theory, the value of polarizability can be calculated by the following sum-over-states expression:[11,30]

$$\alpha_{ij} = 2\sum_{l,k} |\langle k|\mu_i|l\rangle|^2/(E_l - E_k), \quad (1)$$

where l and k stand for the unoccupied (or antibonding) and the occupied (or bonding) orbitals, respectively. The matrix element corresponds to the size of the transition dipole moment. Since α is inversely related to the energy gap, the term that contributes most significantly in sum-over-states expres-

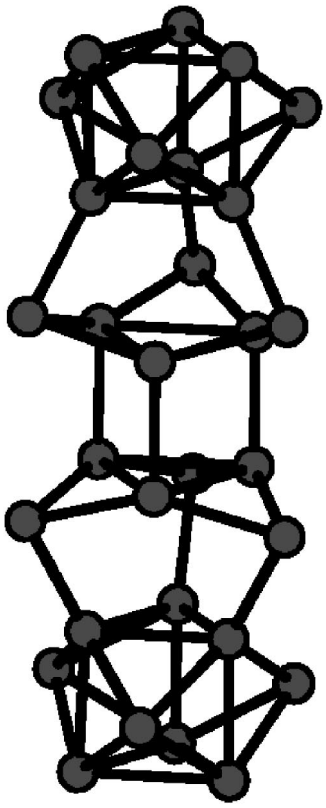

(c) 30E(a(4))

FIG. 1. (*Continued*).

sion would be from those transitions between HOMO and LUMO. Much work has shown that the HOMO-LUMO gap correlates well with the polarizability of a system.[31] As mentioned above, for the closed shell electronic structures, the positive ions would have about the same gaps as their corresponding neutral clusters, but usually not for the negative ions. Therefore the cationic clusters would have closer values of polarizability to those of their corresponding neutral clusters than the anionic clusters. We have reason to think that the differences of the geometries between Si_n and Si_n^- are mainly resulted from their electronic structures.

The binding energy per atom (E_a) for the neutral compact and prolate clusters ($n=24-30$) is shown in Fig. 2. When $n=25$, the compact structure is almost as stable as the prolate structure.[6] For Si_{27}, the two types of structures are degenerate in energy. Although the binding energies E_a's for the prolate structures decrease slightly after n is larger than 27, the E_a's still rise up slowly as the atomic number further increases. We can come to similar conclusions for the cationic clusters. For the anionic clusters, E_a as a function of cluster size n is shown in Fig. 3. Although it is somewhat different from Fig. 2, E_a also increases slowly with cluster size n.

TABLE I. The total binding energies E_b (in eV), their symmetries S, the energy gaps E_g (in eV) between the highest occupied molecular orbital (HOMO) and the lowest unoccupied molecular orbital (LUMO) for Si_n ($n=26-30$) clusters.

Cluster	Si_{26}	Si_{27}	Si_{28}	Si_{29}	Si_{30}
E_b (n(1))	129.637	133.843	139.561	144.773	150.233
S (n(1))	C_s	C_s	C_{2v}	C_{2v}	C_{2v}
E_g (n(1))	1.276	0.720	0.483	0.438	0.366
E_b (n(2))	129.125	133.842	139.027	144.528	149.531
S (n(2))	C_s	C_s	C_s	C_{2v}	C_{2v}
E_g (n(2))	0.899	0.812	1.054	0.747	0.309
E_b (n(3))	128.800	133.647	138.845	144.284	149.477
S (n(3))	C_s	C_{2v}	C_s	C_s	C_{2v}
E_g (n(3))	0.694	0.863	0.619	0.141	0.747
E_b (n(4))	128.173	133.170	138.637	143.741	149.290
S (n(4))	C_s	C_s	C_s	C_s	C_s
E_g (n(4))	0.446	0.792	1.150	0.860	0.094

TABLE II. The total binding energies E_b (in eV), their symmetries S, the energy gaps E_g (in eV) between the highest occupied molecular orbital (HOMO) and the lowest unoccupied molecular orbital (LUMO) for Si_n^- ($n=26-30$) clusters.

Cluster	Si_{26}^-	Si_{27}^-	Si_{28}^-	Si_{29}^-	Si_{30}^-
E_b (a(1))	131.609	136.544	142.432	147.483	152.858
S (a(1))	C_s	D_{3h}	C_{2v}	C_s	C_{2v}
E_g (a(1))	0.710	0.259	0.888	0.446	0.558
E_b (a(2))	131.420	136.395	141.943	147.375	152.153
S (a(2))	C_s	C_s	C_{3v}	C_{2v}	C_{2v}
E_g (a(2))	0.728	0.226	0.933	0.374	0.306
E_b (a(3))	131.326	136.272	141.732	146.617	152.130
S (a(3))	C_s	C_s	C_s	C_{2v}	C_s
E_g (a(3))	0.887	0.411	0.650	0.694	0.460
E_b (a(4))	131.265	136.251	141.268	146.601	152.122
S (a(4))	C_s	C_s	C_s	D_{3h}	C_{2v}
E_g (a(4))	0.430	0.227	0.106	0.294	0.469

TABLE III. The total binding energies E_b (in eV), their symmetries S, the energy gaps E_g (in eV) between the highest-occupied molecular orbital (HOMO) and the lowest unoccupied molecular orbital (LUMO) for Si_n^+ ($n=26-30$) clusters.

Cluster	Si_{26}^+	Si_{27}^+	Si_{28}^+	Si_{29}^+	Si_{30}^+
E_b (c(1))	125.978	130.716	136.254	141.771	147.349
S (c(1))	C_s	C_s	C_{2v}	C_{2v}	C_{2v}
E_g (c(1))	0.648	0.668	0.380	0.444	0.271
E_b (c(2))	125.792	130.663	135.885	141.640	147.323
S (c(2))	C_s	C_s	C_{3v}	C_{2v}	C_{2v}
E_g (c(2))	0.592	0.484	0.437	0.524	0.268
E_b (c(3))	125.646	130.375	135.733	141.355	146.691
S (c(3))	C_s	C_{2v}	C_s	C_{2v}	C_{2v}
E_g (c(3))	0.541	0.766	0.789	0.212	0.322
E_b (c(4))	124.766	130.040	135.460	141.108	146.466
S (c(4))	C_s	C_s	C_s	C_s	C_s
E_g (c(4))	0.337	0.713	0.837	0.541	0.524

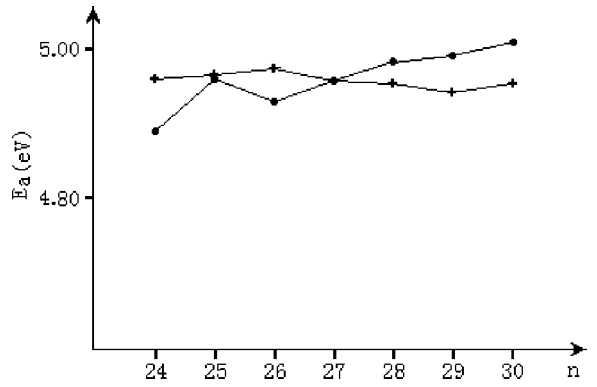

FIG. 2. The binding energies (E_a) of the compact and prolate structures vs the number of atoms for Si_n. Filled circles are for the compact structures. The crosses are for the prolate structures.

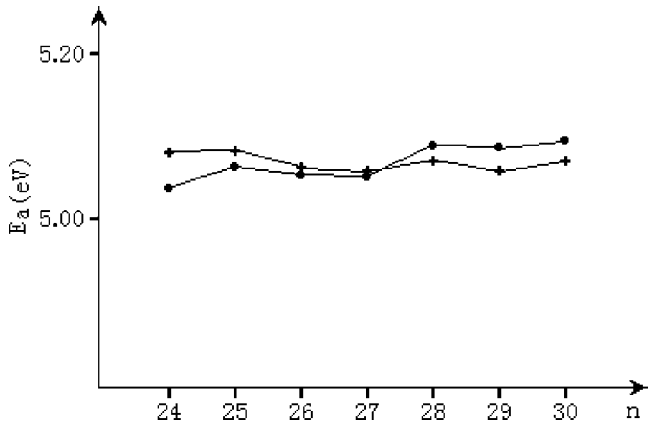

FIG. 3. The binding energies (E_a) of the compact and prolate structures as a function of cluster size n for Si_n^-. Filled circles are for the compact structures. The crosses are for the prolate structures.

According to the discussions above, we find that the compact structures are more stable than the prolate structures starting from $n=28$ for the neutral and ionic clusters. But, the stabilities of the prolate structures do not decrease with the cluster size n over a suitable range. The similar situation can be found in the elongated Si_n ($n=10-50$) clusters discovered by Grossman and Mitáš.[18] Their results suggest that the Si_{10} cluster exhibits high stability in the range from $n=2$ to 23. Starting from $n=25$, the binding energies increase with atomic number. We have investigated another stacked structure consisting of tricapped trigonal prism Si_9 subunits.[29] The binding energies per atom of the Si_n ($n=9+9$, $9+9+9$, $9+9+9+9$, and $9+9+9+9+9$) stacked structures are 4.91, 4.93, 4.97, and 4.98 eV, respectively. Obviously, the binding energies of the stacked structures still increase slowly as the stacked layers increase. However, when the atomic number further increases, they trend towards a saturation, then their stabilities decrease. 45A in Fig. 4 is built from five Si_9 subunits. Its binding energy per atom is 4.98 eV, which is larger than the maximum 4.97 eV of Si_{24-30}. If we add two capping atoms on the two ends of the Si_{45}, the binding energy per atom of the Si_{47} is 5.00 eV. When atomic number is up to 54 or 56, the stacked structures are unstable. 60A in Fig. 4 is another stacked structure with 60 atoms. Its binding energy per atom decreases to 4.98 eV. For the compact structures,

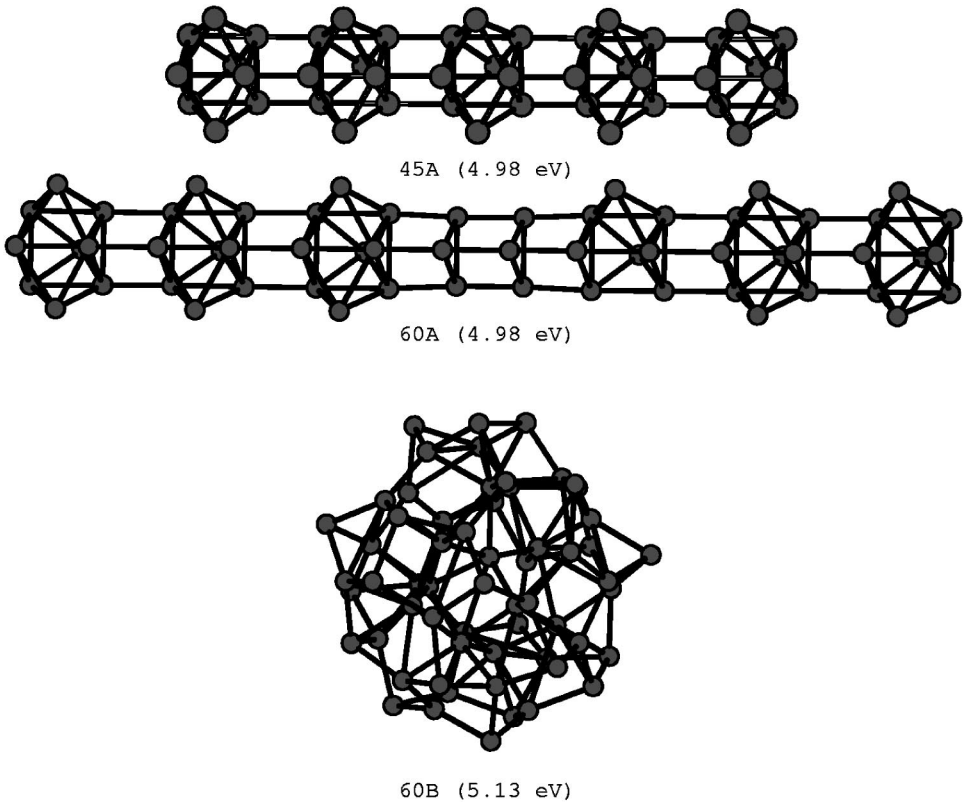

FIG. 4. The prolate structures of Si_{45} and Si_{60} clusters and the near-spherical structure of Si_{60} cluster.

their binding energies increase faster compared with the prolate structures. For example, our calculation shows that the binding energy per atom of the compact Si_{60} (see 60B in Fig. 4) with interior atoms can arrive at 5.13 eV. The total binding energy of 60B is 9.00 eV more than that of 60A.

C, Si, Ge, Sn, and Pb belong to the group IV in the periodic table. Their atomic structures adopt geometries from chain, fullerene cages, and nanotubes for carbon,[32] prolate, and compact structures for Si and Ge,[1,2,6,21] prolate and near-spherical structures for Sn,[33] to compact structures for Pb.[33] For $n \leqslant 7$ and $n=10$ and 12, Si_n, Ge_n, and Sn_n clusters share similar structures. For larger clusters, their ground state structures are different. It is found that the effects of a single charge on the geometries of larger clusters are much less than those on the structures of smaller clusters for Si. This is similar to the situation of Sn clusters.[33]

IV. CONCLUSIONS

The ground state structures for the silicon neutral, anionic, and cationic clusters ranging from 26 to 30 have been obtained using the full-potential linear-muffin-tin-orbital molecular-dynamics (FP-LMTO-MD) method based on the single-parent evolution algorithm. The ground state structures are reported for the first time. We find that Si_n clusters change to the compact structures at $n=27$ from the prolate structures, while the transition occurs at $n=28$ for the charged clusters. For the neutral and ionic clusters, the binding energy ordering may be different. But, generally speaking, the ionic geometries corresponding to the neutral clusters with larger binding energies have usually higher stabilities. As the atomic number increases, the binding energies rise for both the compact structures and the prolate structures. But, the former increases faster than the latter. When the atomic number arrives at a critical size, the stabilities of the prolate structures would decrease.

ACKNOWLEDGMENT

A Foundation for the Author of National Excellent Doctoral Dissertation of People's Republic of China under Grant No. 200320 supported this work.

[1] K. Raghavachari, Phase Transitions **24-26**, 61 (1990).
[2] K. M. Ho, A. A. Shvartsburg, B. Pan, Z. Y. Lu, C. Z. Wang, J. G. Wacker, J. L. Fye, and M. F. Jarrold, Nature (London) **392**, 582 (1998).
[3] C. C. Arnold and D. M. Nuemark, J. Chem. Phys. **99**, 3353 (1993).
[4] E. C. Honea *et al.*, Nature (London) **366**, 42 (1993).
[5] S. Li, R. J. Van Zee, W. Weltner, Jr., and K. Raghavachari, Chem. Phys. Lett. **243**, 275 (1995).
[6] B. X. Li, P. L. Cao, and S. C. Zhan, Phys. Lett. A **316**, 252 (2003).
[7] A. A. Shvartsburg, B. Liu, Z. Y. Lu, C. Z. Wang, M. F. Jarrold, and K. M. Ho, Phys. Rev. Lett. **83**, 2167 (1999).
[8] A. A. Shvartsburg, R. R. Hudgins, P. Dugourd, and M. F. Jarrold, Chem. Soc. Rev. **30**, 26 (2001).
[9] E. Kaxiras and K. Jackson, Phys. Rev. Lett. **71**, 727 (1993).
[10] E. Kaxiras, Phys. Rev. B **56**, 13455 (1997).
[11] C. Pouchan and D. Dégué, J. Chem. Phys. **121**, 4628 (2004).
[12] S. Nigam, C. Majumder, and S. K. Kulshreshtha, J. Chem. Phys. **121**, 7756 (2004).
[13] D. Y. Zhang, D. Bégué, and C. Pouchan, Chem. Phys. Lett. **398**, 283 (2004).
[14] X. L. Zhu and X. C. Zeng, J. Chem. Phys. **118**, 3558 (2003).
[15] X. L. Zhu, X. C. Zeng, and Y. A. Lei, J. Chem. Phys. **120**, 8985 (2004).
[16] C. Majumder and S. K. Kulshreshtha, Phys. Rev. B **69**, 115432 (2004).
[17] S. Yoo, X. C. Zeng, X. Zhu, and J. Bai, J. Am. Chem. Soc. **125**, 13318 (2003).
[18] J. C. Grossman and L. Mitáš, Phys. Rev. B **52**, 16735 (1995).
[19] A. Sieck, Th. Frauenheim, and K. A. Jackson, Phys. Status Solidi B **240**, 537 (2003).
[20] M. F. Jarrold and V. A. Constant, Phys. Rev. Lett. **67**, 2994 (1991).
[21] I. Rata, A. A. Shvartsburg, M. Horoi, T. Frauenheim, K. W. Michael Siu, and K. A. Jackson, Phys. Rev. Lett. **85**, 546 (2000).
[22] M. Methfessel and M. vanSchilfgaarde, Int. J. Mod. Phys. B **7**, 262 (1993).
[23] M. Methfessel and M. vanSchilfgaarde, Phys. Rev. B **48**, 4937 (1993).
[24] M. Methfessel, Phys. Rev. B **38**, 1537 (1988).
[25] M. Methfessel, C. O. Rodriguez, and O. K. Andersen, Phys. Rev. B **40**, 2009 (1989).
[26] O. K. Andersen, Phys. Rev. B **12**, 3060 (1975).
[27] O. K. Andersen and R. G. Woolley, Mol. Phys. **26**, 905 (1975).
[28] M. Springborg and O. K. Andersen, J. Chem. Phys. **87**, 7125 (1975).
[29] B. X. Li, P. L. Cao, R. Q. Zhang, and S. T. Lee, Phys. Rev. B **65**, 125305 (2002).
[30] D. Bégué, M. Merawa, and C. Pouchan, Phys. Rev. A **57**, 2470 (1998).
[31] J. Wang, M. Yang, G. Wang, and J. Zhan, Chem. Phys. Lett. **367**, 448 (2003).
[32] G. von Helden, M. T. Hsu, N. Gotts, and M. T. Bowers, J. Phys. Chem. **97**, 8182 (1993).
[33] C. Majumder, V. Kumar, H. Mizuseki, and Y. Kawazoe, Phys. Rev. B **71**, 035401 (2005).